Turnaround radius in ΛCDM and dark matter cosmologies. II. The role of dynamical friction

Antonino Del Popolo[1,2,*] and Man Ho Chan[3,†]

[1]*Dipartimento di Fisica e Astronomia, University of Catania, Viale Andrea Doria 6, 95125 Catania, Italy*
[2]*Institute of Astronomy, Russian Academy of Sciences, 119017, Pyatnitskaya str., 48, Moscow*
[3]*Department of Science and Environmental Studies, The Education University of Hong Kong, Tai Po, New Territories, Hong Kong*

(Received 16 September 2020; accepted 9 November 2020; published 2 December 2020)

This paper is an extension of the paper by Del Popolo *et al.* [Phys. Rev. D **101**, 083505 (2020)] to take account of the effect of dynamical friction. We show how dynamical friction changes the threshold of collapse δ_c and the turnaround radius R_t. We numerically determine the relationship between the turnaround radius R_t and mass M_t in ΛCDM, dark energy scenarios, and an $f(R)$ modified gravity model. Dynamical friction gives rise to a R_t-M_t relation differing from that of the standard spherical collapse. In particular, dynamical friction amplifies the effects of shear and vorticity already studied by Del Popolo *et al.* A comparison of the R_t-M_t relationships for ΛCDM, dark energy, and modified gravity models shows that the R_t-M_t relationship of ΛCDM is similar to that of the dark energy models, and small differences are seen when comparing with the $f(R)$ models. The effects of shear, rotation, and dynamical friction are particularly evident at galactic scales, giving rise to a difference between the R_t-M_t relation of the standard spherical collapse of the order of $\simeq 60\%$. Finally, we show how the new values of the R_t-M_t relation influence the constraints on the w parameter of the equation of state.

DOI: 10.1103/PhysRevD.102.123510

I. INTRODUCTION

In the past several decades, observations have revealed the existence of missing mass in our Universe [1]. Many physicists believe that the existence of some unknown particles called cold dark matter (CDM) can account for the missing mass [2]. On the other hand, cosmological observations suggest that the expansion of our Universe is accelerating. Many cosmologists have proposed that the existence of a new kind of energy called dark energy can help explain the accelerating expansion [3]. In the standard cosmological model, the amount of dark energy can be represented by the cosmological constant Λ. This standard cosmological model is now known as the ΛCDM model. The ΛCDM model can give good agreement with observations of large-scale structures [4,5]. However, there are some discrepancies between the predictions of the ΛCDM model and the observations of small-scale structures. Specifically, the core-cusp problem [6], missing satellites problem [7], and mass-discrepancy acceleration relation problem [8,9] are three classical problems that challenge the ΛCDM model. Moreover, currently no compelling particle dark matter signal has been detected, either directly or indirectly. The current direct-detection and indirect-detection constraints of dark matter have ruled out a large parameter space of potential particle dark matter models [10–15]. Also, the cosmological constant Λ suffers from the cosmological constant fine-tuning problem and the cosmic coincidence problem [16,17]. Therefore, despite some success on cosmological scales, the ΛCDM model is still challenged by many recent studies.

Based on the above problems, some studies have proposed alternative models for the Universe's accelerated expansion, such as dark energy (DE) effects that are generated by additional matter fields (e.g., quintessence [18]), or that the dynamical effects of dark matter and/or dark energy might originate from modified gravity (MG) models [19–31].

Several popular modified gravity theories have been proposed to compete with the standard ΛCDM model, including emergent gravity [32], $f(R)$ gravity [33], and scalar-tensor-vector gravity [22]. Therefore, it is very important to motivate some theoretical framework to differentiate the dynamical effects of the ΛCDM model and modified gravity models. Some recent studies proposed using the turnaround radius (TAR) to test the standard ΛCDM model and modified gravity models [34–39]. The TAR has been claimed to be a well-defined and unambiguous boundary of a structure (e.g., galaxy clusters)

*adelpopolo@oact.inaf.it
†chanmh@eduhk.hk

in simulations [37]. Different cosmological models and modified gravity models might have different general relations for the TAR. Therefore, precisely determining the TAR of different structures would be crucial to test and constrain different cosmological models [35] and DE, and to disentangle the ΛCDM model, DE, and MG models [34–39].

Contrary to the previous claim, we already showed in Refs. [40–45] that shear and vorticity modify the nonlinear evolution of structures. In this paper, we will also show that dynamical friction further modifies the structure formation, and consequently modifies the TAR, and that the TAR generally depends on baryon physics [45]. By using an extended spherical collapse model, the TAR depends on the effects of shear and vorticity. Taking into account the effects of shear and vorticity, the relation between the TAR and total mass can differ by 30% from that when these effects are omitted, especially in galaxies [45]. In the present paper, we show that the effect of dynamical friction is also significant.

The TAR was calculated in Refs. [37,38] for the ΛCDM model, while Ref. [39] obtained the TAR in generic gravitational theories.

In this paper, we extend the results of Ref. [45], based on an extended spherical collapse model (ESCM) introduced and adopted in Refs. [4,40,42–44]. The ESCM takes into account the effects of shear, vorticity, and dynamical friction on the collapse to show how the TAR is changed. Apart from the typical parameters of spherical collapse, the shear, vorticity, and dynamical friction change the two-point correlation function [46], the weak lensing peaks [44], and the mass function [4,40,42,43]. Similarly to Ref. [45], the aim of this paper is to show how the parameters of the spherical collapse are changed, together with the R_t-M_t relation for MG and DE models, and to compare with ΛCDM model predictions.

The paper is organized as follows. Section II describes the model used to derive the R_t-M_t relation. Section III is devoted to the discussion of our results. Section IV is devoted to conclusions.

II. THE MODEL

In the following, we will use an improved version [47–53] of the spherical collapse model introduced in Ref. [54]. The model describes the evolution of perturbations from the linear to the nonlinear phase, when they decouple from the Hubble flow, reach a maximum radius, reach the TAR, collapse, and virialize to form a structure. The initial model of Ref. [54] was extended to take account of angular momentum [50,52,53,55–62], dynamical friction [63,64], shear [65–67], and the effects of the DE fluid perturbation [see [68–76]]. The effects of shear and rotation have been studied in smooth DE models [40,41], clustering DE cosmologies [77], and Chaplygin cosmologies [78].

A. The ESCM

Here, we show how to obtain the evolution equations of δ in the nonlinear regime.

The evolution equations of δ in the nonlinear regime were obtained in Refs. [70,79–83]. In order to obtain the equations, we use the neo-Newtonian expressions for the relativistic Poisson equation, Euler equation, and continuity equations [84]:

$$\frac{\partial\rho}{\partial t}+\nabla_{\vec{r}}\cdot(\rho\vec{v})+\frac{P}{c^2}\nabla_{\vec{r}}\cdot\vec{v}=0, \tag{1}$$

$$\frac{\partial\vec{v}}{\partial t}+(\vec{v}\cdot\nabla_{\vec{r}})\vec{v}+\nabla_{\vec{r}}\Phi+\frac{\mathbf{c}^2}{\mathbf{c}^2\rho+\mathbf{P}}\nabla\mathbf{P}=0, \tag{2}$$

$$\nabla^2\Phi-4\pi G\left(\rho+\frac{3P}{c^2}\right)=0, \tag{3}$$

where the equation of state (EoS) is given by $P=w\rho c^2$, where $\vec{r}$ is the physical coordinate, Φ is the Newtonian gravitational potential, and $\vec{v}$ is the velocity in three-space. Writing and combining the perturbation equation as in Ref. [45], we obtain the nonlinear evolution equation in a dust ($w=0$) universe,

$$\ddot{\delta}+2H\dot{\delta}-\frac{4}{3}\frac{\dot{\delta}^2}{1+\delta}-4\pi G\bar{\rho}\delta(1+\delta)-(1+\delta)(\sigma^2-\omega^2)=0. \tag{4}$$

Equation (4) is Eq. 41 of Ref. [81], and a generalization of Eq. 7 of Ref. [70] to the case of a nonspherical configuration of a rotating fluid.

In Eq. (4), H is the Hubble function, $\bar{\rho}=\rho-\delta\rho$ is the background density, and $\sigma^2=\sigma_{ij}\sigma^{ij}$ and $\omega^2=\omega_{ij}\omega^{ij}$ are the shear and rotation terms, respectively. The shear term is related to a symmetric traceless tensor dubbed the shear tensor, while the rotation term is related to an antisymmetric tensor.

In terms of the scale factor a, the nonlinear equation driving the evolution of the overdensity contrast can be rewritten as

$$\delta''+\left(\frac{3}{a}+\frac{E'}{E}\right)\delta'-\frac{4}{3}\frac{\delta'^2}{1+\delta}-\frac{3}{2}\frac{\Omega_{\mathrm{m},0}}{a^5E^2(a)}\delta(1+\delta)-\frac{1}{a^2H^2(a)}(1+\delta)(\sigma^2-\omega^2)=0, \tag{5}$$

where $\Omega_{m,0}$ is the DM density parameter at $t=0$ ($a=1$) and $E(a)$ is given in Eq. 11 of Ref. [45].

Since $\delta=\frac{2GM_{\mathrm{m}}}{\Omega_{m,0}H_0^2}(a/R)^3-1$, where R is the effective perturbation radius, by inserting this into Eq. (4) it is easy to check that the evolution equation for δ reduces to the spherical collapse model (SCM) [81,85,86],

$$\ddot{R} = -\frac{GM_{\rm m}}{R^2} - \frac{GM_{\rm de}}{R^2}(1+3w_{\rm de}) - \frac{\sigma^2-\omega^2}{3}R = -\frac{GM_{\rm m}}{R^2} - \frac{4\pi G\bar{\rho}_{\rm de}R}{3}(1+3w_{\rm de}) - \frac{\sigma^2-\omega^2}{3}R, \quad (6)$$

where $M_{\rm de}$ is the mass of the dark-energy component enclosed in the volume, $M_{\rm m} = \frac{4\pi R^3}{3}(\bar{\rho}+\delta\rho)$, and $w_{\rm de}$ and $\bar{\rho}_{\rm de}$ are the DE equation-of-state parameter and its background density, respectively [44,81,85,86].

In the case $w = -1$, namely, the cosmological constant case Eq. (6) can be written as

$$\ddot{R} = -\frac{GM_{\rm m}}{R^2} - \frac{\sigma^2-\omega^2}{3}R + \frac{\Lambda}{3}R. \quad (7)$$

The previous equation is clearly similar to the usual expression for the SCM with a cosmological constant and angular momentum [e.g., [59,62,87]]:

$$\frac{d^2R}{dt^2} = -\frac{GM}{R^2} + \frac{L^2}{M^2R^3} + \frac{\Lambda}{3}R = -\frac{GM}{R^2} + \frac{4}{25}\Omega^2 R + \frac{\Lambda}{3}R. \quad (8)$$

The rightmost term in Eq. (8) is obtained by recalling that $L = I\Omega$, where the moment of inertia of a sphere $I = 2/5MR^2$.

Angular momentum is related to vorticity by $\Omega = \omega/2$ (see also Ref. [88]) in the case of uniform rotation with angular velocity $\Omega = \Omega_z \mathbf{e}_z$. As in Refs. [40,41,45], we define the dimensionless but mass-dependent quantity α as the ratio between the rotational and gravitational terms in Eq. (8):

$$\alpha(M) = \frac{L^2}{M^3RG}. \quad (9)$$

In order to solve Eq. (4), the relation between the term $\sigma^2-\omega^2$ and the density contrast δ is needed. This connection can be obtained by recalling the relation between angular momentum and shear, and recalling that Eq. (8) (from which α was obtained) is equivalent to Eq. (6), which is also equivalent to Eq. (4).

Calculating the same ratio between the gravitational and extra terms appearing in Eq. (4), we obtain

$$\frac{\sigma^2-\omega^2}{H_0^2} = -\frac{3}{2}\frac{\alpha\Omega_{\rm m,0}}{a^3}\delta. \quad (10)$$

This reasonable assumption (see Ref. [41]) was also used in Refs. [40–43].

The nonlinear equation to solve is obtained by substituting Eq. (10) into Eq. (4),

$$\ddot{\delta} + 2H\dot{\delta} - \frac{4}{3}\frac{\dot{\delta}^2}{1+\delta} - 4\pi G\bar{\rho}\delta(1+\delta) - \frac{3}{2}H_0^2(1+\delta)\frac{\alpha\Omega_{\rm m,0}}{a^3}\delta = 0. \quad (11)$$

By solving Eq. (11) following the method described in Ref. [83] or by solving Eq. (6), the threshold of collapse and the turnaround can be obtained.

At this point, we also want to take into account dynamical friction in our analysis. Then, we notice that Eq. (6) can be written in a more general form by taking into account dynamical friction [63,64,87,89–96],

$$\ddot{R} = -\frac{GM}{R^2} + \frac{L^2(R)}{M^2R^3} + \frac{\Lambda}{3}R - \eta\frac{{\rm d}R}{{\rm d}t} = -\frac{GM_{\rm m}}{R^2} - \frac{GM_{\rm de}}{R^2}(1+3w_{\rm de}) - \frac{\sigma^2-\omega^2}{3}R - \eta\frac{dR}{dt}, \quad (12)$$

where η is the dynamical friction coefficient. Equation (12) can be obtained via Liouville's theorem [46], and the dynamical friction force per unit mass $\eta\frac{{\rm d}R}{{\rm d}t}$ was given in Ref. [64] (Appendix D, Eq. D5) and Ref. [95] (Eq. 5).

A similar equation (excluding the dynamical friction term) was obtained by several authors (e.g., Refs. [41,85,86]) and generalized to smooth DE models in Ref. [44].

Equations (12) and (6) differ due to the presence of the dynamical friction term. Similarly to rotation and the cosmological constant, dynamical friction delays the collapse of a structure (perturbation) [63,64,95–97]. The magnitudes of the effects of the cosmological constant, rotation, and dynamical friction are of the same order, with differences of a few percent (see Fig. 1 of Ref. [97] and Fig. 11 of Ref. [64]).

Notice that, by means of the relation $\delta = \frac{2GM_{\rm m}}{\Omega_{m,0}H_0^2}(a/R)^3 - 1$, Eq. (12) can be written in terms of δ, similarly to Eq. (4).

Our SCM model depends not only on shear and vorticity (as in Ref. [45]), but also on dynamical friction. Since shear, rotation, and dynamical friction depend on mass, the SCM results depend on the baryon physics, which is different from what was claimed in Refs. [34,35,37].

III. RESULTS

The effects of shear [65–67] and rotation [41,44,46,93,98–100] on the collapse are manifold.

One general feature is that of slowing down the collapse [99–102]. The mass function [41–44,46,97,98], two-point correlation function [103], and scaling relations like the mass-temperature and luminosity-temperature relations [96,103,104] are modified. This is connected to the change of the typical parameters of the SCM.

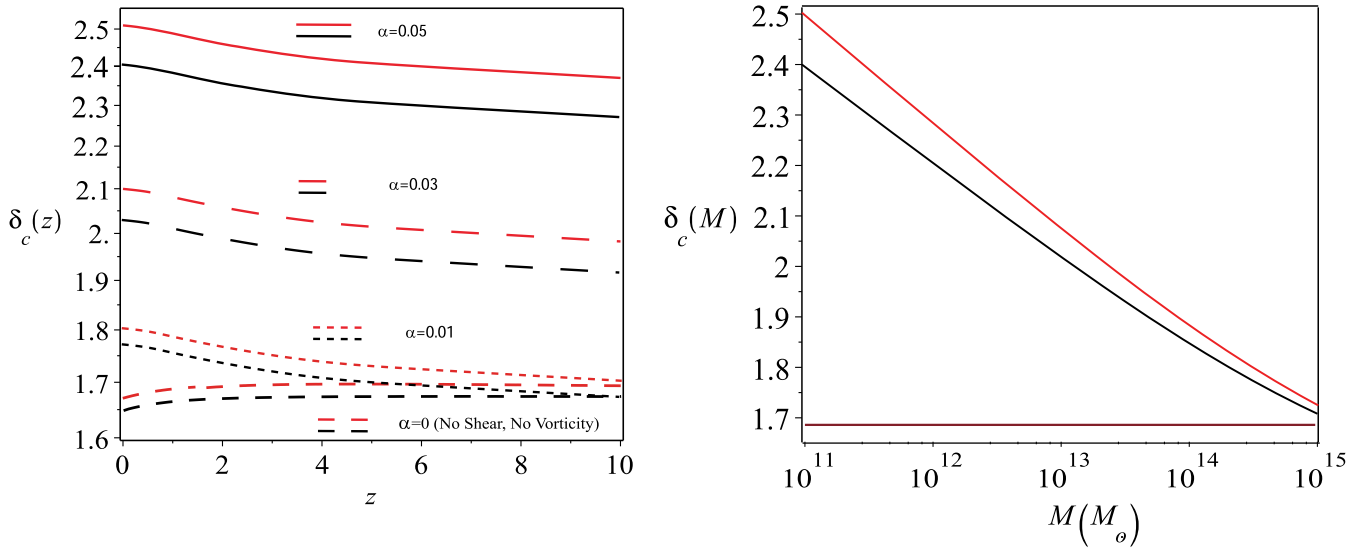

FIG. 1. The threshold of collapse δ_c as a function of redshift and mass. Left: δ_c vs redshift. The predictions for $\delta_c(z)$ for the ΛCDM model are represented by the red lines. The values of α are 0.05 (solid line) (galactic mass scale), 0.03 (long dashed line), 0.01 (dotted line) (cluster mass scale), and 0 (dashed line). Right: δ_c vs mass. The solid red line represents the result of the ESCM model, the red dashed line that of the elliptical collapse model of Ref. [106], and the brown line the ΛCDM expectation when shear and rotation are not taken into account.

A. Threshold of collapse with shear, rotation, and dynamical friction

Figure 1 shows how shear, rotation, and dynamical friction (hereafter, SRD) change the collapse threshold δ_c. We show the dependence on redshift and mass in the left and right panel, respectively. The red line represents the predictions of the ESCM for $\delta_c(z)$ for the ΛCDM model, while the black line shows the ESCM in the case of one DE model: the Albrecht-Skordis (AS) model [105].

In the left panel, from top to bottom, the values of α are 0.05 (solid line) corresponding to a mass $\simeq 10^{11}\,M_\odot$, 0.03 (long dashed line) corresponding to a mass $\simeq 10^{13}\,M_\odot$, 0.01 (dotted line) corresponding to a mass $\simeq 10^{15}\,M_\odot$, and 0 (dashed line). The value of $\delta_c(z)$ for $\alpha = 0.05$ is $\simeq 30\%$ larger than in the $\alpha = 0$ case.

In the case of no shear, rotation ($\alpha = 0$), and dynamical friction, δ_c has a weak dependence on redshift in the z range [0, 2] and then assumes the value predicted by the Einstein–de Sitter model.

In other terms, SRD gives rise to a nonflat threshold δ_c, which is monotonically decreasing with redshift. Moreover, the larger is α, the larger is the difference between the values of $\delta_c(z)$, as shown by the different curves.

Of the DE quintessence models in the literature, we plotted the AS model because the other models considered in previous papers [40,83] [INV1 ($w_0 = -0.4$), INV2 ($w_0 = -0.79$), 2EXP ($w_0 = -1$), CNR ($w_0 = -1$), CPL ($w_0 = -1$), and SUGRA ($w_0 = -0.82$) (see Refs. [41,83])[1]] are contained in the envelope between the region included in the ΛCDM and AS models (see Fig. 4 of Ref. [83]).

The right panel of Fig. 1 plots $\delta_c(M)$ vs mass. In the absence of SRD the value of δ_c is constant (brown line), while in the presence of SRD δ_c becomes mass dependent and monotonically decreases with mass. This means that in order a less massive perturbation (e.g., galaxies) form structures must cross a higher threshold than more massive ones. This behavior is related to the anticorrelation of the angular momentum acquired by the proto-structure and its height.[2] Since low peaks acquire larger angular momentum than high peaks, they need a higher density contrast to collapse and form structures [64,93,99–102,108].

As shown in the left and right panels of Fig. 1, the effect of dynamical friction is to increase the values of $\delta_c(z)$ and $\delta_c(M)$ with respect to the case when it is not present, as shown in Ref. [45].

B. Comparison of TAR in the ΛCDM, ESCM, and DE models

Shear, rotation, and dynamical friction modify the TAR. In order to show this, we may compare the predictions of the ΛCDM, ESCM, and DE models. References [37,38] calculated the maximum TAR (MTAR), that is, the radius of the surface where $\ddot{R} = 0$. Reference [38] found

[1] w_0 is the value of w today.

[2] The peak height is defined as $\nu = \delta_c/\sigma(M)$, where $\sigma(M)$ is the mass variance. The specific angular momentum j is given by $j \propto \nu^{-3/2}$ [64,65,107].

$$R_{\rm ta} = \left[\frac{-3M}{4\pi\rho_{\rm de}(1+3w)}\right]^{1/3}, \tag{13}$$

which in the case of the ΛCDM model ($w=-1$) reduces to [37]

$$R_{\rm ta} = \left[\frac{3GM}{\Lambda}\right]^{1/3}. \tag{14}$$

In their estimation, they assumed that shear and rotation were not present. Their expression can be generalized to the case where shear and rotation are nonzero. This can be done by using Eq. (6) to obtain

$$R_{\rm ta} = \left[\frac{-3M}{4\pi\rho_{\rm de}(1+3w)+(\sigma^2-\omega^2)}\right]^{1/3}. \tag{15}$$

In this paper, we will calculate and plot the TAR, not the MTAR, since we compare with Ref. [35] which calculated the TAR.

Figure 2 shows the TAR predicted by the ΛCDM model (solid red line), the ESCM model (taking into account shear rotation and dynamical friction) for the ΛCDM model (red dashed line), and the AS model (black dashed line). When shear, rotation, and dynamical friction are taken into account the collapse is slowed down and the TAR is smaller. The difference between the ΛCDM model and the ESCM predictions increases when going towards smaller masses. This is mainly related to the larger rotation of smaller objects, and reaches a maximum difference of ≃60%. The black dashed line (as already reported) is the AS model, which has a slightly larger TAR with respect to the ΛCDM model.

C. Constraints on the DE EoS parameter

Knowing the relation between the TAR, structure mass, and EoS parameter, it is possible to obtain some constraints on the DE EoS (w). This was attempted in Ref. [38] by means of Eq. (13). In general, a great number of DE models are described through the equation of state parameter $w(a)$. This depends on its present value w_0, its value at the matter-radiation equality epoch, and some other parameters at the same epoch (see Eq. 23 of Ref. [83]). If one wants to constrain the evolution of the EoS parameter w, high-redshift structures are needed. Conversely, is one wants to constrain the values of w_0, small-z cosmic structures may be used. Reference [38] compared the predicted TARs at different values of w in the M_t-R_t plane, finding constraints on w_0. To this aim, data from several structures (e.g., the Milky Way, M81/M82 group, Local Group, Virgo cluster, and Fornax-Eridanus group) were used. It is of fundamental importance to note that the constraints depend on the model used. As shown in Ref. [109], the mass of the structure and its TAR changes when the cosmological constant is added to the standard SCM (considering only the gravitational potential) (Eq. 1 of Ref. [109]). This was also pointed out comparing the values predicted by several Karachentsev's paper (e.g., Refs. [110,111] for M81, the local group, and neighboring groups) with those of Ref. [109].

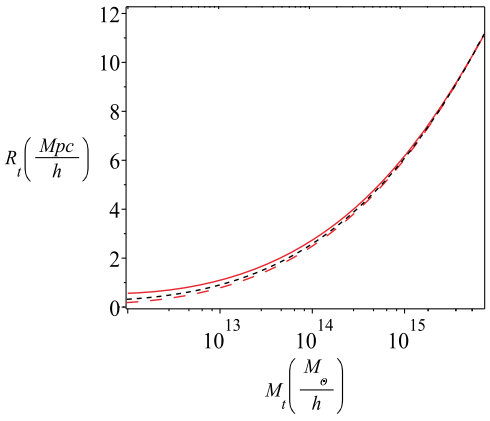

FIG. 2. Turnaround radius $R_{\rm t}$ vs mass $M_{\rm t}$. The solid red line represents the TAR predicted by the standard SCM, and the dashed red line shows the ESCM result for the ΛCDM model. The black dotted line is the result of the ESCM for the AS model.

In Fig. 3 the solid lines obtained from the TAR equation (13) correspond (from bottom to top) to $w=-2.5$, -2, -1.5, -1, and -0.5 when shear, rotation, and dynamical friction are absent. The dashed lines are the corrections obtained when shear, rotation, and dynamical friction are taken into account. The range of w for which no stable structures exist is given by the parameter space above each line. Reference [38] discussed some constraints on w based on the highest mass objects. As shown by the dashed lines, one has to expect that at masses smaller than $10^{13}\,M_\odot$ the TAR is modified by the presence of shear, rotation, and dynamical friction. As a consequence, structures at smaller masses can give different constraints on w. At the same time, following Ref. [109], by taking the effect of dynamical friction into account we see that the constraints on the cosmic structure plotted in Fig. 3 are notably different from that of Ref. [45]. The values of the TAR and mass for each of the objects in Fig. 3 were obtained using the SCM with dynamical friction, and using a method described in Refs. [109,112] (see the Appendix). In Table I we report the constraints we obtained.

D. Comparison with the TAR in $f(R)$ theories

In this section, we compare the evolution of the TAR in the ESCM and the $f(R)$ theories. The evolution of the TAR in general relativity (GR) and in the $f(R)$ theories was investigated in Ref. [35]. MG effects were introduced in the overdensity evolution equation (their Eq. 3.3) by means of the parameter $\epsilon(a,k)$, where k is the (angular) wave number. GR is recovered when $\epsilon(a,k)$ is zero, and our Eq. (5) is recovered in the case when $\epsilon(a,k)$ is zero and shear and rotation are set equal to zero. In other terms, our Eq. (5) is a generalization of Eq. 3.3 of Ref. [35] for the

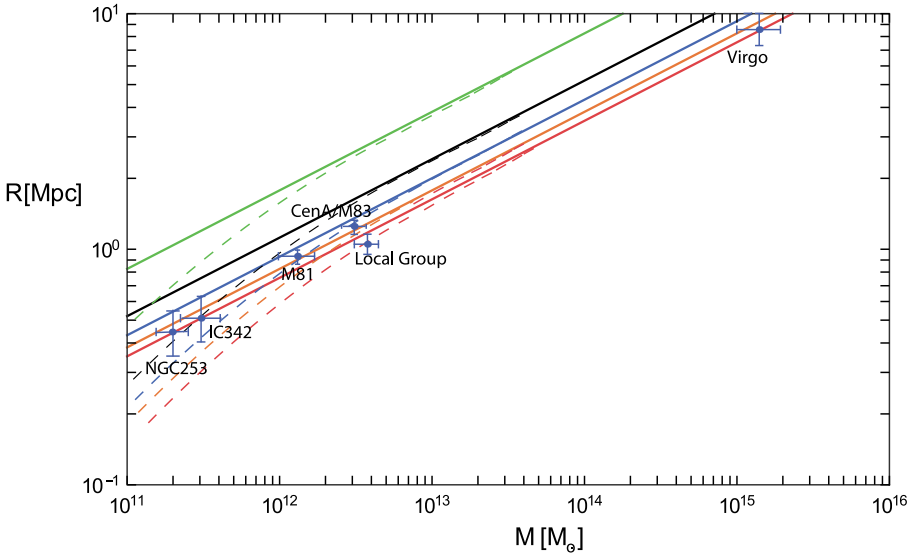

FIG. 3. Stable structure mass-radius relation for different w. The solid lines from top to bottom represent $w = -0.5$ (green), -1 (black), -1.5 (blue), -2 (pink), and -2.5 (red). The results of the ESCM are represented by the dashed lines. The dots with error bars are data from Ref. [38].

case where $\epsilon(a, k)$ is zero. Consequently, their Figs. 1 and 3 (similarly to the left panel of our Fig. 1, and to the ΛCDM, and DE models without shear and rotation, as shown in Ref. [83]) shows a monotonic increase of $\delta_c(z)$. Their Fig. 4 shows an almost flat behavior of $\delta_c(M)$, with variations from constancy of the order of 1%. The behavior of $\delta_c(z)$ and $\delta_c(M)$ in Ref. [35] disagrees with the predictions of several papers (e.g., Refs. [40–43,97,106]). The previous papers showed that in order to have a mass function that reproduces the results of simulations, the threshold must be a monotonically decreasing function of mass. Since in Ref. [35] $\delta_c(M)$ was practically constant and $\delta_c(z)$ was a monotonically increasing function of redshift, their results cannot reproduce the mass function obtained in simulations and observations. This is due to the fact that Ref. [35] discarded the effects of shear and rotation, and in general of aspericities. A more detailed discussion of this aspect can be found in Ref. [45].

Going back to our main goal, namely, the use of the TAR to distinguish GR-MG and GR-DE models (e.g., Ref. [35]), we will compare the prediction of Ref. [35] for the M_t-R_t relation with that of our ESCM. In Fig. 4 we plot the results obtained in Ref. [35] for R_t vs mass for the ΛCDM model, the model with $\epsilon = 1/3$, and $f(R)$ with $f_{R0} = 10^{-6}$, 10^{-5}, and 10^{-4}. The 68% confidence level region of our prediction for the ΛCDM model obtained with the ESCM is represented by the grey band. The 68% confidence level was obtained (as in Ref. [45]) by means of a Monte Carlo simulation. The result of the plot is slightly different from Fig. 4 of Ref. [45]. Because of the presence of dynamical friction, which further contributes to slowing down the collapse, the TAR has smaller values. Consequently, the TAR in the ESCM model does not completely overlap with that of Ref. [35], as happened in Ref. [45]. This means that the study of the highest values of the M_t-R_t relation could disentangle the GR predictions from those of the $f(R)$ theories. Choosing peculiar values of the TAR would be possible to distinguish between GR and $f(R)$ theories.

TABLE I. The allowed ranges of w based on the ESCM model.

Stable structure	Range of w
M81	$w \geq -1.5$
IC342	$w \geq -1$
NGC253	$w \geq -1$
CenA/M83	$w \geq -1.5$
Local Group	$w \geq -2$
Virgo	$w \geq -2$

In Fig. 5 the predictions of some of the quintessence DE models previously cited are compared to the same $f(R)$ models of Ref. [35] plotted in Fig. 4. All of the curves are obtained by means of the ESCM applied to the DE models of the TAR. From top to bottom, the cyan, blue, brown, magenta, black, red, and green lines represent results from INV1, INV2, SUGRA, w_{09},[3] AS, ΛCDM without shear and rotation, and ΛCDM with shear and rotation, respectively.

A comparison of the predictions from Ref. [35] for the TAR with those of the DE models is plotted in the right panel. In this plot, we show only INV2 (blue dashed line) and the ΛCDM with shear, rotation, and dynamical friction (green dashed line). With the exception of INV1, the two quoted curves contain all other DE models.

[3]Namely, the model with $w = -0.9$.

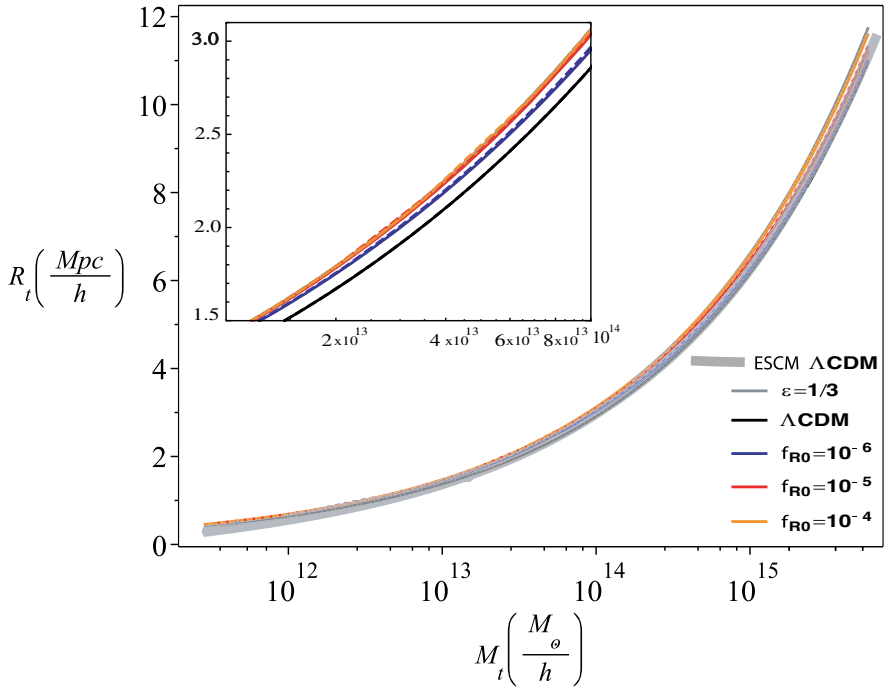

FIG. 4. Turnaround radius R_t vs mass M_t. The plot represents the result obtained in Ref. [35] for R_{ta} vs mass for the ΛCDM model, the model with $\epsilon = 1/3$, and $f(R)$ with $f_{R0} = 10^{-6}$, 10^{-5}, and 10^{-4}. The gray band represents the 68% confidence level region of our prediction for the ΛCDM model obtained with the ESCM.

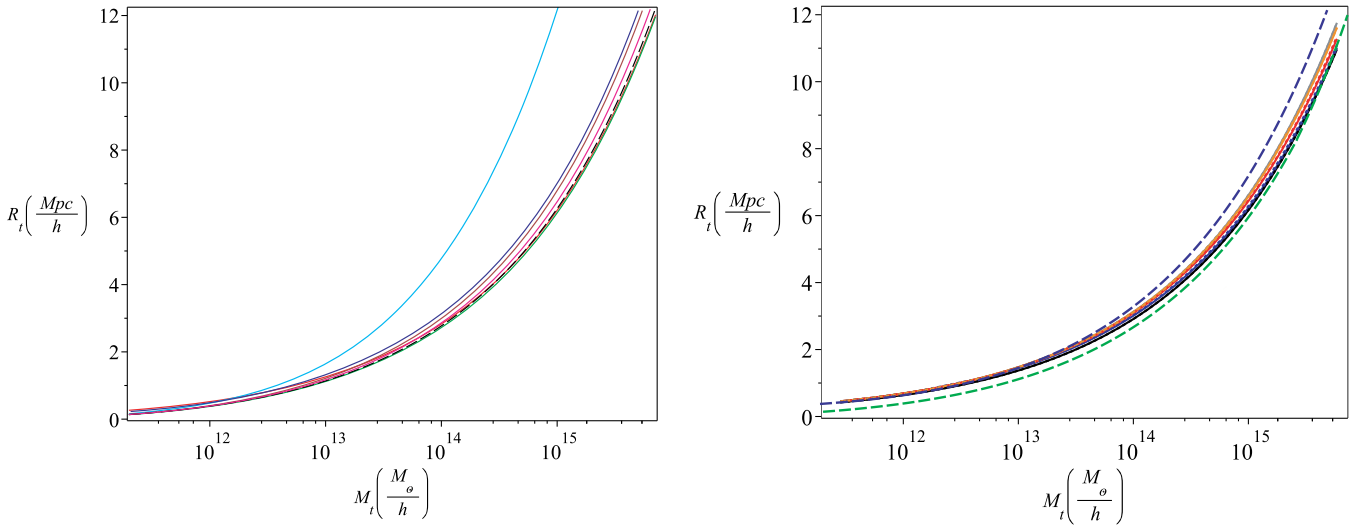

FIG. 5. The turnaround radius R_t vs mass M_t obtained with the ESCM for the DE models. Left: from top to bottom, the cyan, blue, brown, magenta, black, red, and green lines represent the results for INV1, INV2, SUGRA, w_{09} (namely, the model with $w = -0.9$), AS, ΛCDM without shear, and rotation, and ΛCDM with shear and rotation, respectively. Right: the solid lines are the results for the ΛCDM and $f(R)$ models of Ref. [35], while the blue dashed and green dashed lines are for the INV2 model and the ΛCDM with shear, rotation, and dynamical friction plotted in the left panel.

The other lines are the ΛCDM and $f(R)$ models of Ref. [35]. Differently from Fig. 4, the DE models contain the TAR prediction from Ref. [35]. As a consequence, the TAR cannot be used to distinguish between DE and $f(R)$ theory predictions.

IV. CONCLUSIONS

In this paper we discussed how shear, rotation, and dynamical friction change the TAR and some of the parameters of the SCM. The results were obtained using an ESCM taking into account the effects of shear, vorticity,

and dynamical friction to determine the R_t-M_t relation in ΛCDM and DE scenarios. We numerically extended the formula for the maximum TAR obtained in Ref. [45] to take into account dynamical friction. The value of the TAR is reduced by shear, rotation, and dynamical friction, especially at galactic scales. Using the R_t-M_t relationship and data from stable structures, one can obtain constraints on w. Its values are smaller for structures with masses approximately smaller than $10^{13}\,M_\odot$. In this paper we recalculated the mass and TAR of the M81/M82 group, Local Group, Virgo cluster, NGC253, IC342, and CenA/M83 group following Refs. [109,112].

A comparison of the R_t-M_t relationship obtained for ΛCDM and DE scenarios with the prediction from Ref. [35] of the $f(R)$ theories shows that the R_t-M_t relationships in the $f(R)$ models are practically identical to those of DE scenarios. This implies that the R_t-M_t relationship is not a good probe to distinguish between GR and DE model predictions. The situation is different in the case of the ΛCDM model. In this case, the 68% confidence level region does not overlap with that of the $f(R)$ models. The higher values of the TAR could be used to distinguish between $f(R)$ theories and GR.

APPENDIX: MASS AND TAR OF STRUCTURES

The most general equation that takes into account shear, rotation, and dynamical friction is Eq. (12). We will rewrite it in an adimensional form. We assume that $J = kR^\alpha$, with $\alpha = 1$ (in agreement with Ref. [113].[4]), and that k is constant. In terms of the variables $y = R/R_0$ and $t = x/H_0$, Eq. (12) can be written as

$$\frac{d^2y}{dx^2} = -\frac{A}{2y^2} + \Omega_\Lambda y + \frac{K_j}{y} - \frac{\eta}{H_0}\frac{dy}{dx}, \tag{A1}$$

where $K_j = k\frac{1}{(H_0R_0)^2}$,[5] $A = \frac{2GM}{H_0^2R_0^3}$, and

$$H = H_0\sqrt{\left(\frac{a_0}{a}\right)^3\Omega_m + \Omega_\Lambda}. \tag{A2}$$

Equation (A1) has a first integral, given by

$$u^2 = \left(\frac{dy}{dx}\right)^2 = \frac{A}{y} + \Omega_\Lambda y^2 + 2K_j\log y - 2\frac{\eta}{H_0}\int\left(\frac{dy}{dx}\right)^2 dx + K, \tag{A3}$$

where $K = \frac{2E}{(H_0R_0)^2}$ and E is the energy per unit mass of a shell.

[4]In that paper, $\alpha = 1.1 \pm 0.3$.
[5]$K_j = 0.78$ and $\frac{\eta}{H_0} = 0.5$.

The previous equation can solved as described in Refs. [109,112].

The mass and turnaround radius of some groups of galaxies are obtained by finding a relation between the velocity, and radius, v-R. The later will be fitted to the data. The v-R relation is obtained as follows. Let us consider Fig. 6. This is a solution of Eq. (12) for different values of K. The vertical line corresponds to $x = 0.964$. Its intersection with the curves, solution of Eq. (12) (cyan, red, green) gives, for each one a value $y(x) = y(0.964)$. The solution of Eq. (12), also gives the velocity, allowing us to find $u(x) = u(0.964)$. We get a couple of values (y, u) for each intersection of the vertical line with the curves. This allows us to find a series of points that can be fitted with a relation of the form $u = -b/y^n + by$, which gives $u = -1.3436/y^{0.9107} + 1.3436y$. This last relation can be written in physical units as follows:

$$v(R) = -bH_0R_0\left(\frac{R_0}{R}\right)^n + bH_0R. \tag{A4}$$

Substituting $R_0 = (\frac{2GM}{H_0^2})^{\frac{1}{3}}$ into this equation, we get

$$v(R) = -b\frac{H_0}{R^n}\left(\frac{2GM}{AH_0^2}\right)^{\frac{n+1}{3}} + bH_0R \tag{A5}$$

or

$$v(R) = -\frac{-0.66385H_0}{R^n}\left(\frac{GM}{H_0^2}\right)^{\frac{n+1}{3}} + 1.3436H_0R, \tag{A6}$$

where $n = 0.9107$. Equation (A6) satisfies the condition $v(R_0) = 0$. Fitting the equation to the data of Ref. [112] (Fig. 2) and Ref. [109] (Fig. 2), one obtains the value of the Hubble parameter H_0 and the TAR. By solving Eq. (12) one can obtain the value of A, and by solving the equation $A = \frac{2GM}{H_0^2R_0^3}$ one gets the mass M.

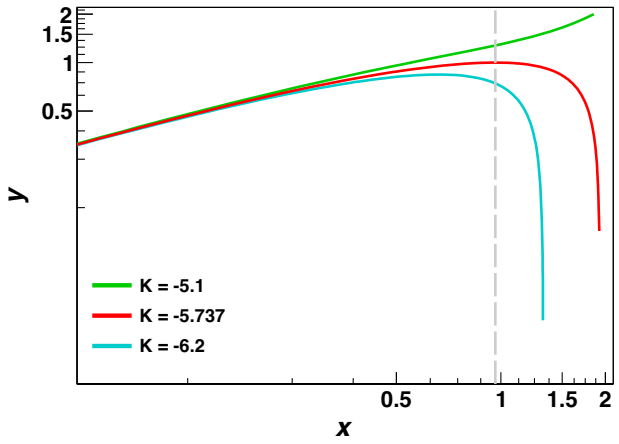

FIG. 6. Evolution of shell radius for different values of K. The red, cyan, and green lines correspond to $K = -5.737$, $K = -6.2$, and $K = -5.1$, respectively.

[1] R. H. Sanders, *The Dark Matter Problem: A Historical Perspective* (Cambridge University Press, Cambridge, England, 2010).
[2] S. Profumo, *An Introduction to Particle Dark Matter* (World Scientific, Singapore, 2017).
[3] M. Li, X.-D. Li, S. Wang, and Y. Wang, Commun. Theor. Phys. **56**, 525 (2011).
[4] A. Del Popolo, AIP Conf. Proc. **1548**, 2 (2013).
[5] P. A. R. E. A. Ade, Astron. Astrophys. **594**, A13 (2016).
[6] W. J. G. de Blok, Adv. Astron. **2010**, 1 (2010).
[7] B. Moore, S. Ghigna, F. Governato, G. Lake, and T. Quinn, Astrophys. J. **524**, L19 (1999).
[8] S. S. McGaugh, Astrophys. J. **609**, 652 (2004).
[9] S. S. McGaugh, F. Lelli, and J. M. Schombert, Phys. Rev. Lett. **117**, 201101 (2016).
[10] E. E. A. Aprile, Phys. Rev. Lett. **119**, 181301 (2017).
[11] D. E. A. Abecrcrombie, Phys. Dark Universe **27**, 100371 (2020).
[12] M. E. A. Ackermann, Phys. Rev. Lett. **115**, 231301 (2015).
[13] M. H. Chan and C. H. Leung, Sci. Rep. **7**, 14895 (2017).
[14] M. H. Chan, L. Cui, J. Liu, and C. S. Leung, Astrophys. J. **872**, 177 (2019).
[15] M. H. Chan and C. M. Lee, Phys. Rev. D **102**, 063017 (2020).
[16] S. Weinberg, Rev. Mod. Phys. **61**, 1 (1989).
[17] H. E. S. Velten, R. F. vom Marttens, and W. Zimdahl, Eur. Phys. J. C **74**, 3160 (2014).
[18] E. J. Copeland, M. Sami, and S. Tsujikawa, Int. J. Mod. Phys. D **15**, 1753 (2006).
[19] G. W. Horndeski, Int. J. Theor. Phys. **10**, 363 (1974).
[20] M. Milgrom, Astrophys. J. **270**, 365 (1983).
[21] B. Zwiebach, Phys. Lett. B **156**, 315 (1985).
[22] J. W. Moffat, J. Cosmol. Astropart. Phys. 3 (2006) 004.
[23] S. Nojiri, S. D. Odintsov, and M. Sasaki, Phys. Rev. D **71**, 123509 (2005).
[24] J. D. Bekenstein, Modified gravity as an alternative to dark matter, in *Particle Dark Matter: Observations, Models and Searches*, edited by G. Bertone (Cambridge University Press, Cambridge, England, 2010), p. 99.
[25] A. De Felice and S. Tsujikawa, Living Rev. Relativity **13**, 3 (2010).
[26] E. V. Linder, Phys. Rev. D **81**, 127301 (2010).
[27] M. Milgrom, Phys. Rev. D **89**, 024027 (2014).
[28] D. Lovelock, J. Math. Phys. (N.Y.) **12**, 498 (1971).
[29] P. Hořava, Phys. Rev. D **79**, 084008 (2009).
[30] Y. Rodríguez and A. A. Navarro, J. Phys. Conf. Ser. **831**, 012004 (2017).
[31] C. Deffayet, O. Pujolàs, I. Sawicki, and A. Vikman, J. Cosmol. Astropart. Phys. 10 (2010) 026.
[32] E. P. Verlinde, SciPost Phys. **2**, 016 (2017).
[33] H. A. Buchdahl, Mon. Not. R. Astron. Soc. **150**, 1 (1970).
[34] S. Bhattacharya, K. F. Dialektopoulos, A. Enea Romano, C. Skordis, and T. N. Tomaras, J. Cosmol. Astropart. Phys. 7 (2017) 018.
[35] R. C. C. Lopes, R. Voivodic, L. R. Abramo, and L. Sodré, Jr., J. Cosmol. Astropart. Phys. 09 (2018) 010.
[36] R. C. C. Lopes, R. Voivodic, L. R. Abramo, and L. Sodré, Jr., J. Cosmol. Astropart. Phys. 07 (2019) 026.
[37] V. Pavlidou and T. N. Tomaras, J. Cosmol. Astropart. Phys. 09 (2014) 020.
[38] V. Pavlidou, N. Tetradis, and T. N. Tomaras, J. Cosmol. Astropart. Phys. 05 (2014) 017.
[39] V. Faraoni, M. Lapierre-Léonard, and A. Prain, J. Cosmol. Astropart. Phys. 10 (2015) 013.
[40] A. Del Popolo, F. Pace, and J. A. S. Lima, Int. J. Mod. Phys. D **22**, 1350038 (2013).
[41] A. Del Popolo, F. Pace, and J. A. S. Lima, Mon. Not. R. Astron. Soc. **430**, 628 (2013).
[42] F. Pace, R. C. Batista, and A. Del Popolo, Mon. Not. R. Astron. Soc. **445**, 648 (2014).
[43] A. Mehrabi, F. Pace, M. Malekjani, and A. Del Popolo, Mon. Not. R. Astron. Soc. **465**, 2687 (2017).
[44] F. Pace, C. Schimd, D. F. Mota, and A. D. Popolo, J. Cosmol. Astropart. Phys. 19 (2019) 060.
[45] A. Del Popolo, M. H. Chan, and D. F. Mota, Phys. Rev. D **101**, 083505 (2020).
[46] A. Del Popolo and M. Gambera, Astron. Astrophys. **344**, 17 (1999).
[47] J. A. Fillmore and P. Goldreich, Astrophys. J. **281**, 1 (1984).
[48] E. Bertschinger, Astrophys. J. Suppl. Ser. **58**, 39 (1985).
[49] Y. Hoffman and J. Shaham, Astrophys. J. **297**, 16 (1985).
[50] B. S. Ryden and J. E. Gunn, Astrophys. J. **318**, 15 (1987).
[51] K. Subramanian, R. Cen, and J. P. Ostriker, Astrophys. J. **538**, 528 (2000).
[52] Y. Ascasibar, G. Yepes, S. Gottlöber, and V. Müller, Mon. Not. R. Astron. Soc. **352**, 1109 (2004).
[53] L. L. R. Williams, A. Babul, and J. J. Dalcanton, Astrophys. J. **604**, 18 (2004).
[54] J. E. Gunn and J. R. Gott III, Astrophys. J. **176**, 1 (1972).
[55] A. V. Gurevich and K. P. Zybin, Zh. Eksp. Teor. Fiz. **94**, 3 (1988).
[56] A. V. Gurevich and K. P. Zybin, Zh. Eksp. Teor. Fiz. **94**, 5 (1988).
[57] S. D. M. White and D. Zaritsky, Astrophys. J. **394**, 1 (1992).
[58] P. Sikivie, I. I. Tkachev, and Y. Wang, Phys. Rev. D **56**, 1863 (1997).
[59] A. Nusser, Mon. Not. R. Astron. Soc. **325**, 1397 (2001).
[60] N. Hiotelis, Astron. Astrophys. **382**, 84 (2002).
[61] M. Le Delliou and R. N. Henriksen, Astron. Astrophys. **408**, 27 (2003).
[62] P. Zukin and E. Bertschinger, in *APS Meeting Abstracts* (2010) p. 13003.
[63] V. Antonuccio-Delogu and S. Colafrancesco, Astrophys. J. **427**, 72 (1994).
[64] A. Del Popolo, Astrophys. J. **698**, 2093 (2009).
[65] Y. Hoffman, Astrophys. J. **308**, 493 (1986).
[66] Y. Hoffman, Astrophys. J. **340**, 69 (1989).
[67] S. Zaroubi and Y. Hoffman, Astrophys. J. **416**, 410 (1993).
[68] D. F. Mota and C. van de Bruck, Astron. Astrophys. **421**, 71 (2004).
[69] N. J. Nunes and D. F. Mota, Mon. Not. R. Astron. Soc. **368**, 751 (2006).
[70] L. R. Abramo, R. C. Batista, L. Liberato, and R. Rosenfeld, J. Cosmol. Astropart. Phys. 11 (2007) 12.
[71] L. R. Abramo, R. C. Batista, L. Liberato, and R. Rosenfeld, Phys. Rev. D **77**, 067301 (2008).

[72] L. R. Abramo, R. C. Batista, and R. Rosenfeld, J. Cosmol. Astropart. Phys. 7 (2009) 40.
[73] L. R. Abramo, R. C. Batista, L. Liberato, and R. Rosenfeld, Phys. Rev. D **79**, 023516 (2009).
[74] P. Creminelli, G. D'Amico, J. Noreña, L. Senatore, and F. Vernizzi, J. Cosmol. Astropart. Phys. 3 (2010) 27.
[75] T. Basse, O. Eggers Bjælde, and Y. Y. Y. Wong, J. Cosmol. Astropart. Phys. 10 (2011) 38.
[76] R. C. Batista and F. Pace, J. Cosmol. Astropart. Phys. 6 (2013) 44.
[77] F. Pace, R. C. Batista, and A. Del Popolo, Mon. Not. R. Astron. Soc. **445**, 648 (2014).
[78] A. Del Popolo, F. Pace, S. P. Maydanyuk, J. A. S. Lima, and J. F. Jesus, Phys. Rev. D **87**, 043527 (2013).
[79] F. Bernardeau, Astrophys. J. **433**, 1 (1994).
[80] T. Padmanabhan, *Current Applied Physics*, edited by T. Padmanabhan (1996).
[81] Y. Ohta, I. Kayo, and A. Taruya, Astrophys. J. **589**, 1 (2003).
[82] Y. Ohta, I. Kayo, and A. Taruya, Astrophys. J. **608**, 647 (2004).
[83] F. Pace, J.-C. Waizmann, and M. Bartelmann, Mon. Not. R. Astron. Soc. **406**, 1865 (2010).
[84] J. A. S. Lima, V. Zanchin, and R. Brandenberger, Mon. Not. R. Astron. Soc. **291**, L1 (1997).
[85] P. Fosalba and E. Gaztañaga, Mon. Not. R. Astron. Soc. **301**, 503 (1998).
[86] S. Engineer, N. Kanekar, and T. Padmanabhan, Mon. Not. R. Astron. Soc. **314**, 279 (2000).
[87] P. J. E. Peebles, *Princeton Series in Physics, Princeton*, edited by P. J. E. Peebles (Princeton University Press, NJ, 1993).
[88] A. D. Chernin, Astron. Astrophys. **267**, 315 (1993).
[89] A. Kashlinsky, Astrophys. J. **306**, 374 (1986).
[90] A. Kashlinsky, Astrophys. J. **312**, 497 (1987).
[91] O. Lahav, P. B. Lilje, J. R. Primack, and M. J. Rees, Mon. Not. R. Astron. Soc. **251**, 128 (1991).
[92] J. G. Bartlett and J. Silk, Astrophys. J. Lett. **407**, L45 (1993).
[93] A. Del Popolo and M. Gambera, Astron. Astrophys. **337**, 96 (1998).
[94] A. Del Popolo, M. Gambera, and V. Antonuccio-Delogu, Astron. Astrophys. **16**, 127 (1998).
[95] A. Del Popolo, Astron. Astrophys. **454**, 17 (2006).
[96] A. Del Popolo, F. Pace, and D. F. Mota, Phys. Rev. D **100**, 024013 (2019).
[97] A. Del Popolo, F. Pace, and M. Le Delliou, J. Cosmol. Astropart. Phys. 3 (2017) 032.
[98] A. Del Popolo and M. Gambera, Astron. Astrophys. **357**, 809 (2000).
[99] A. Del Popolo, E. N. Ercan, and Z. Xia, Astron. J. **122**, 487 (2001).
[100] A. Del Popolo, Astron. Astrophys. **387**, 759 (2002).
[101] P. J. E. Peebles, Astrophys. J. **365**, 27 (1990).
[102] E. Audit, R. Teyssier, and J.-M. Alimi, Astron. Astrophys. **325**, 439 (1997), arXiv:astro-ph/9704023.
[103] A. Del Popolo, N. Hiotelis, and J. Peñarrubia, Astrophys. J. **628**, 76 (2005).
[104] A. Del Popolo, Mon. Not. R. Astron. Soc. **336**, 81 (2002).
[105] A. Albrecht and C. Skordis, Phys. Rev. Lett. **84**, 2076 (2000).
[106] R. K. Sheth, H. J. Mo, and G. Tormen, Mon. Not. R. Astron. Soc. **323**, 1 (2001).
[107] E. Polisensky and M. Ricotti, Mon. Not. R. Astron. Soc. **450**, 2172 (2015).
[108] B. S. Ryden, Astrophys. J. **329**, 589 (1988).
[109] S. Peirani and J. A. de Freitas Pacheco, Astron. Astrophys. **488**, 845 (2008).
[110] I. D. Karachentsev, A. E. Dolphin, D. Geisler, E. K. Grebel, P. Guhathakurta, P. W. Hodge, V. E. Karachentseva, A. Sarajedini, P. Seitzer, and M. E. Sharina, Astron. Astrophys. **383**, 125 (2002).
[111] I. D. Karachentsev, Astron. J. **129**, 178 (2005).
[112] S. Peirani and J. A. de Freitas Pacheco, Nature (London) **11**, 325 (2006).
[113] J. S. Bullock, T. S. Kolatt, Y. Sigad, R. S. Somerville, A. V. Kravtsov, A. A. Klypin, J. R. Primack, and A. Dekel, Mon. Not. R. Astron. Soc. **321**, 559 (2001).